metals

MDPI

Article

Numerical Modelling of the Influence of Argon Flow Rate and Slag Layer Height on Open-Eye Formation in a 150 Ton Steelmaking Ladle

Eshwar Kumar Ramasetti [1,*], Ville-Valtteri Visuri [1], Petri Sulasalmi [1], Timo Fabritius [1], Jari Savolainen [2], Mingming Li [3] and Lei Shao [3]

1 Process Metallurgy Research Unit, University of Oulu, PO Box 4300, 90014 Oulu, Finland; ville-valtteri.visuri@oulu.fi (V.-V.V.); petri.sulasalmi@oulu.fi (P.S.); timo.fabritius@oulu.fi (T.F.)
2 Outokumpu Stainless Oy, Terästie, 95490 Tornio, Finland; jari.savolainen@outokumpu.com
3 School of Metallurgy, Northeastern University, Heping District, Shenyang 11004, China; limm@smm.neu.edu.cn (M.L.); shaolei@smm.neu.edu.cn (L.S.)
* Correspondence: eshwar.ramasetti@oulu.fi; Tel.: +358-503507332

Received: 17 August 2019; Accepted: 25 September 2019; Published: 26 September 2019

Abstract: A transient computational fluid dynamics (CFD) modelling approach was used to study the complex multi-phase flow in an argon-stirred industrial scale ladle with a nominal capacity of 150 tons. During the stirring process, when gas was injected through the porous plug from the bottom into the steel bath, it breaks up into bubbles and infringes the slag layer creating an open-eye. The volume of fluid model was used to investigate the open-eye formation process in the simulations. In the numerical simulations, the open-eye area changed from 0.7 to 2.24 m^2 with the increment of argon flow rate from 200 to 500 NL/min for slag layer thickness of 40 cm. Furthermore, the influence of slag layer height on the open-eye area was investigated. An argon flow rate of 200 NL/min was able to break the slag layer for slag layer height of 40 cm, and the open-eye formation was not possible for the same flow rate when the slag layer height was elevated from 40 to 55 cm. The numerical simulation results were validated against industrial measurements carried out at Outokumpu Stainless located in Tornio, Finland. The numerical simulation results of dynamics and time-averages of the slag area showed a good agreement when compared to the industrial measurements. To conclude, it is necessary to define gas flow rate based on the slag layer height to have an open-eye suitable for alloying.

Keywords: ladle metallurgy; open-eye formation; slag layer; CFD

1. Introduction

In ladle metallurgy, gas stirring is largely used to homogenize the composition of alloy elements, temperature in the molten steel, and to remove inclusions. Gas stirring is typically carried out by injecting argon into the steel through the porous plug or nozzle. The gas breaks into bubbles forming a buoyant plume which, consequently, induces a circulating flow of steel in the ladle. The behavior of the slag layer during the stirring process plays a pivotal role in refining the molten steel as the efficiency of the chemical reactions between the slag-steel phases depends on the interaction between them. To encourage the rate of refining reactions between steel and slag, gas stirring is exploited in order to break the slag layer and promote emulsification of slag into the steel. In certain processes, the slag layer is broken to form an open-eye to expose the steel surface for feeding purposes. On the other hand, the formation of a larger open-eye may end up in capturing oxygen from the atmosphere into the liquid steel, which is disadvantageous to the steel quality.

Over the past few decades, open-eye formation has been studied in water-scale models [1–23] and industrial-scale ladles [24–29]. Water-modelling studies [1–6] have focused on investigating the effect of flow rate and slag layer height on the open-eye formation under the conditions of kinematic and dynamic similarity with an industrial ladle. Furthermore, the measurements performed by Lv et al. [7], Amaro-Villeda et al. [8], and Maruyama and Iguchi [9] studied the effect of slag layer height on the open-eye size. Mazumdar et al. [10–17] contributed to a greater extent towards investigating the fluid-flow analysis and open-eye formation process through experiments and simulations. Furthermore, the work was also extended by developing the models for calculating dimensionless open-eye area and mixing phenomena in ladles. Recently, Li et al. [18–22] performed both experiments and simulations to study the formation of open-eye process and slag/steel/gas interface shape for various flow rates in a water model ladle. Ramasetti et al. [23,26] also performed both experiments and numerical simulations in a 1/5 scale water model for investigating the influence of gas flow rate and slag layer height on the open-eye area with single and dual-plug configurations.

Overall, for the industrial ladle there are not many experimental measurements of open-eye formation available in the literature when compared to the water model ladle. This is due to the difficult conditions (e.g., high temperatures, process gases and dust) on the ladle surface, which make it quite hard to capture the process with a video camera. During the past few years, Valentin et al. [24] captured the open-eye formation process in a 170-ton industrial ladle and studied the effect of stirring rate on it. Li et al. [25] modelled the complex multi-phase flow in an industrial scale ladle using the volume of fluid (VOF) model. The open-eye diameter changed from 0.43 to 0.81 m with the elevation of argon flow rate from 100 to 300 NL/min in the simulations. The open-eye diameter enlarged from 0.67 to 0.87 m, when the argon flow rate was elevated from 200 to 500 NL/min from the simulation results of Liu et al. [26].

Liu et al. [26] also investigated the effect of plug configuration on the open-eye area and mixing phenomena. Cloete et al. [27,28] used discrete particle model (DPM) and volume of fluid (VOF) models to study the effect of design variables on the mixing efficiency in an industrial scale gas stirred ladle. Recently, Liu et al. [29] performed simulations using the large eddy simulation (LES) approach coupled with VOF and DPM for both a water model and an industrial ladle.

Over the past few years, the studies have concentrated more on modelling water-model ladles and there have been relatively few studies on modelling industrial ladles through experiments and simulations. In the current work, the influence of gas flow rate and slag layer height on open-eye formation was investigated through industrial measurements and numerical simulations. The industrial measurements were conducted at Outokumpu Stainless Oy located in Tornio, Finland. As for the simulation part, the VOF model was used to investigate the slag/steel/gas behavior in the ladle.

2. Mathematical Model

2.1. Governing Equations

In the present work, a VOF model is used to solve the complex multi-phase flow three-phase and to investigate the slag/steel/gas interface behavior in the industrial-scale ladle. The governing equations of the VOF model and standard $k-\varepsilon$ turbulence model are described below [30].

Equations (1) and (2) presents the continuity and momentum equations solved in the current work.

$$\frac{\partial \rho}{\partial t} + \frac{\partial (\rho u_i)}{\partial x_i} = 0 \tag{1}$$

$$\frac{\partial (\rho u_i)}{\partial t} + \frac{\partial \left(\rho u_i u_j\right)}{\partial x_j} = -\frac{\partial p}{\partial x_i} + \frac{\partial}{\partial x_j}\left[\mu_{\text{eff}}\left(\frac{\partial u_i}{\partial x_j} + \frac{\partial u_j}{\partial x_i}\right)\right] + F_i + F_{vol}, \tag{2}$$

where ρ is the density, u_i is the fluid flow velocity, p is the pressure, μ_e is the viscosity, g_i is the gravitational acceleration, F_i is the body force and F_{vol} is the volume force, given by:

$$F_i = \alpha \rho_l g_i, \tag{3}$$

$$F_{vol} = \sigma_{ij} \frac{\rho \kappa_i \nabla \alpha_i}{\frac{1}{2}\left(\rho_i + \rho_j\right)} \tag{4}$$

A more detailed description of the VOF and standard $k-\varepsilon$ model used in the current work can be found in earlier studies [23,31].

2.2. Physical Properties and Operating Condictions

The industrial scale ladle studied in this work is a 150 ton ladle. The physical properties and operating conditions used in the current work are shown in Table 1.

Table 1. Thermo-physical properties and operating conditions employed.

Physical Properties at 1812 K	Value	Unit
Density of liquid steel [32]	6913	kg/m^3
Viscosity of liquid steel [32]	0.005281	Pa·s
Density of slag	2746	kg/m^3
Viscosity of slag	0.081	Pa · s
Density of argon gas	0.8739	kg/m^3
Viscosity of argon gas	2.2616×10^{-5}	Pa · s
Temperature of bath	1812	K
Flow rate of argon gas	200, 400 and 500	NL/min *
Slag layer height	25, 40 and 55	cm

* Normal temperature and pressure (NTP): 293.15 K and 101325 Pa.

2.3. Execution of the Experiments

The industrial measurements were performed with gas flow rates ranging from 200 to 500 NL/min and slag layer thickness varying from 25 to 55 cm. Slag layer thickness was measured manually using a steel rod. An infrared (IR) camera from Sapotech Oy was used to monitor the open-eye formation and evolution in the industrial ladle operated at very high temperature. The open software ImageJ software was used to analyze the open-eye size.

2.4. Initial and Boundary Conditions

At the start of the gas-stirring process, the steel and slag are at rest with no gas injection from the porous plug at the bottom. Heat transfer was excluded from the simulations. Instead, it was assumed that the argon gas immediately heats up to the temperature of the liquid steel (1812 K). Accordingly, the velocity inlet boundary condition in the simulations was computed by the argon gas flow rates by Equation (5).

$$V_{\text{in}} = \frac{Q_{\text{L}}}{A} = \left(\frac{p_{\text{S}}}{p_{\text{L}}}\frac{T_{\text{R}}}{T_{\text{T}}}\right)\frac{Q_{\text{S}}}{A} \tag{5}$$

where subscript R is the ladle operating condition and T is the standard condition. T_{S} = 293.15 K, T_{L} = 1812 K, p_{S} = 101,325 Pa, and $p_{\text{L}} = p_{\text{S}} + \rho_{\text{steel}} g H$. A is the porous plug area, and Q_{S} is the measured argon gas flow rate at normal temperature and pressure (NTP). It should be noted that Equation (5) does not account for the pressure head caused by top slag, as it is very small compared to that of the steel bath.

2.5. Employed Physical Properties of Slag

The average slag composition (excluding minor amounts of Cr_2O_3, Ni, S and P) was 61.3 wt% CaO, 26.0 wt% SiO_2, 7.8 wt% MgO, 0.2 wt% MnO, 4.3 wt% Al_2O_3 and 0.4 wt% Fe_2O_3. The composition

was determined based on four slag samples taken from the process studied, while the employed average slag temperature represents an average of the temperatures measured during the validation experiments. For the sake of simplicity, the top slag was assumed to be liquid. The viscosity of the slag was calculated using the viscosity module of FactSage ver. 7.2. [33]. The viscosity module relates the dynamic viscosity of the slag to the structure of the slag melt, which is calculated using the modified quasichemical model [30]. The density of the slag was calculated using the partial molar volume method using Equations (6) and (7) [34].

$$\rho_{\text{slag}} = \frac{M_{\text{slag}}}{V_{\text{m,slag}}}, \tag{6}$$

$$V_{\text{m,slag}} = \sum_{i=0}^{n} x_i \overline{V_i}, \tag{7}$$

where M_{slag} is the molar mass of the slag, $V_{\text{m,slag}}$ is the molar volume of slag, x_i is the molar fraction of species i in slag and $\overline{V_i}$ is the partial molar volume of species i in the slag. The values of $\overline{V_i}$ at 1500 °C (1773 K) were taken from [31]; the error induced from using the same values for the temperatures of this work was assumed to be small. The dynamic viscosity and density of the slag were calculated based on an average slag composition and at a temperature of 1539 °C (1812.15 K).

2.6. Numerical Details

The geometry, computational domain and boundary conditions of the ladle configuration studied is shown in Figure 1. A completely hexahedral structured mesh for the ladle was created using the blocking feature of ANSYS ICEM computational fluid dynamics (CFD) software (version 17, Espoo, Finland). The number of cells was approximately 1 million cells. The criteria used in the earlier studies of Ramasetti et al. [23,31] is used in the present work.

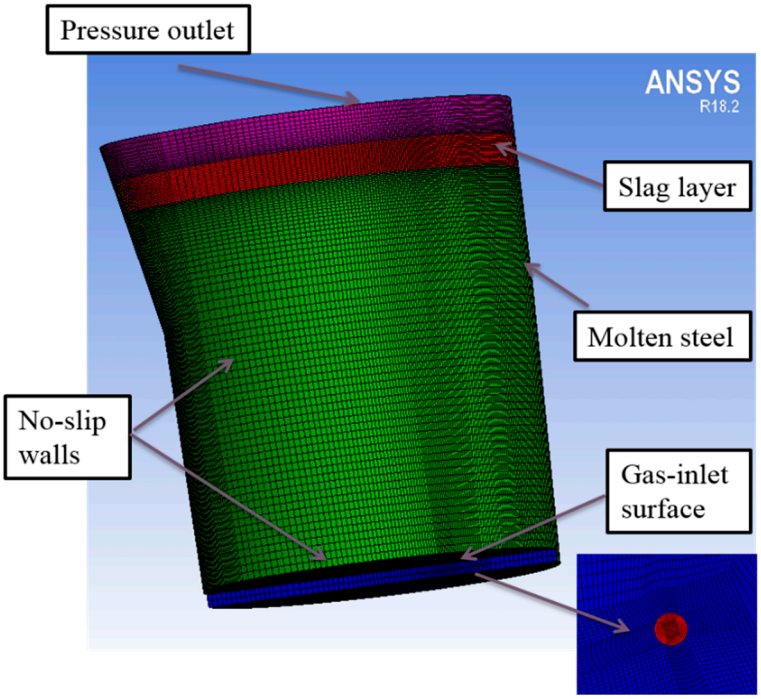

Figure 1. The geometry, mesh and boundary conditions of the ladle studied.

3. Results and Discussion

3.1. Influence of Argon Flow Rate on Open-Eye Formation for Slag Layer Thickness of 40 cm

Figures 2 and 3 show the argon gas propagation and the open-eye formation process at the initial stages of gas stirring for flow rates of 200 and 500 NL/min. The argon gas, which was injected into the bath through the nozzle, splits up into bubbles and impinge the slag layer at high flow rates forming a open-eye. Figures 2 and 3 show that the upwelling argon gas appears to be continuous and concentrated before breaking the slag layer. The time taken for the argon gas to reach the slag layer appears to be shorter for a flow rate of 500 NL/min (see Figure 2) in comparison to 200 NL/min (Figure 3). At 3.0 s physical time, the argon gas was already able to break the slag layer and the open-eye formation can be observed for a flow rate of 500 NL/min (see Figure 3b), while for a flow rate of 200 NL/min the open-eye is not completely formed (see Figure 2b).

(**a**) At time = 1.5 sec (**b**) At time = 3.0 sec (**c**) At time = 4.5 sec

Figure 2. The argon gas floating and open-eye formation process: Q = 200 NL/min.

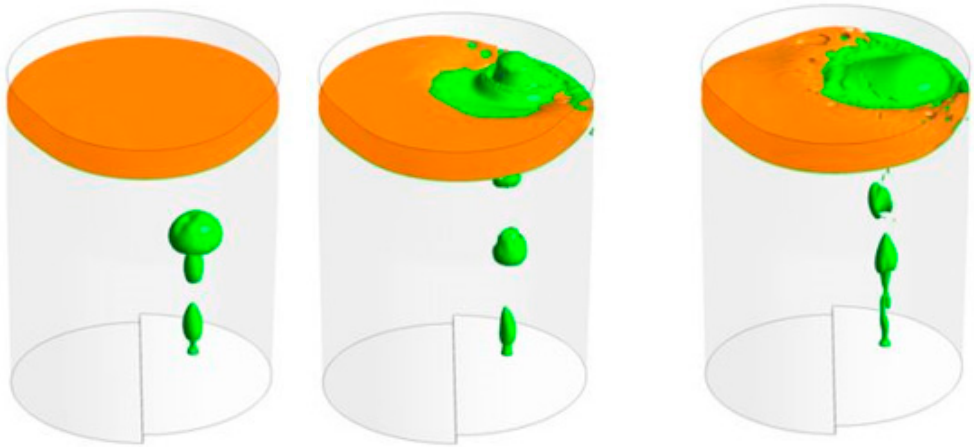

(**a**) At time = 1.5 sec (**b**) At time = 3.0 sec (**c**) At time = 4.5 sec

Figure 3. The argon gas floating and open-eye formation process: Q = 500 NL/min.

The influence of argon flow rate on the open-eye area for a slag layer thickness of 40 cm is displayed in Figures 4 and 5 from the experimental and simulation results. The position and size of the open-eye generated was not constant throughout the process; the value of the open-eye area was averaged over a period of 60 s. The argon flow rate of 200 NL/min was able to break the slag layer and generate a smaller open-eye with an area of 0.7 m^2 (relative area of 10.3%) in experiments (Figure 4a)

and 0.69 m^2 (relative area of 10.2%) through simulations (Figure 5a). The open-eye formation did not appear when the industrial scale ladle operated with a flow rate lesser than 200 NL/min. For a flow rate of 400 NL/min, the open-eye area generated was approximately 1.58 m^2 (relative area of 23.3%) in experiments (Figure 4b) and 1.59 m^2 (relative area of 23.5%) through simulations. At a flow rate of 500 NL/min, the area of the open-eye was 2.24 m^2 (relative area of 33.1%) in experiments (Figure 4c) and 2.3 m^2 (relative area of 34.0%) through simulations (Figure 5c). At higher flow rates, the edge of the open-eye moves closer to the ladle wall, resulting in an increase of fluid flow adjacent to the ladle wall. This may increase refractory wear and thus diminish the ladle life. The predicted trend of increase in the open-eye area with argon flow rate were in acceptable agreement with the industrial observations of Valentin et al. [24]. The simulation results of the open-eye area accorded well with the simulations of Li et al. [25] and Liu et al. [26]. This information can be used to select the optimal argon flow rates to achieve a sufficient-sized open-eye for alloying purposes.

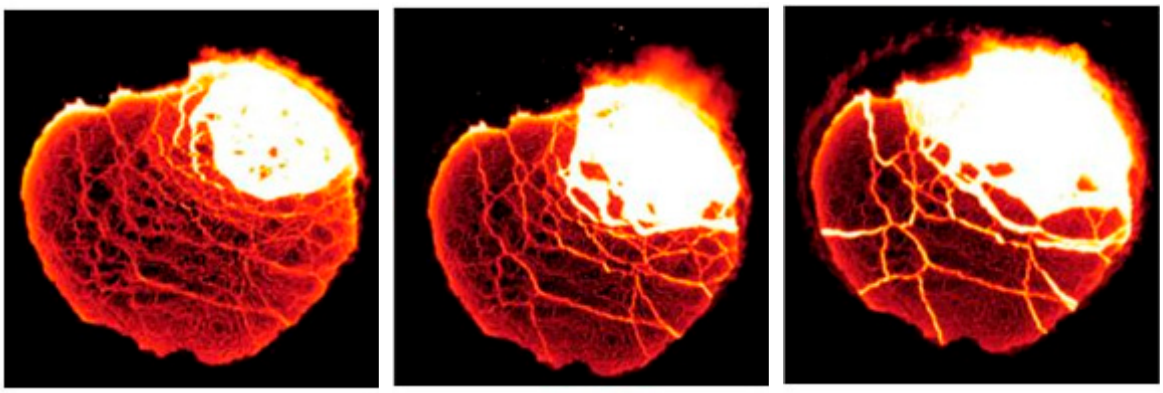

(**a**) (**b**) (**c**)

Figure 4. Open-eye size in the ladle from experimental results for a slag layer thickness of 40 cm: (**a**) Q = 200 NL/min, (**b**) Q = 400 NL/min, and (**c**) Q = 500 NL/min.

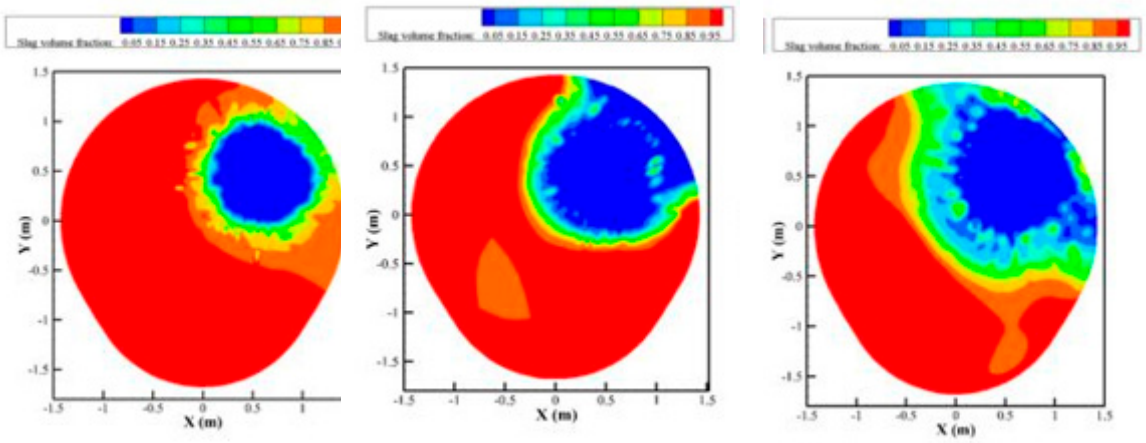

(**a**) (**b**) (**c**)

Figure 5. Open-eye size in the ladle from simulation results for a slag layer thickness of 40 cm: (**a**) Q = 200 NL/min, (**b**) Q = 400 NL/min, and (**c**) Q = 500 NL/min.

Figure 6 depicts the fluctuation of the open-eye area with time for flow rates of 200, 400 and 500 NL/min. It can be observed that the open-eye area is regularly changing, indicating the dynamic behavior of the slag layer. Initially, the open-eye expands rapidly and the area reaches a peak value that is dependent of the flow rate (see Figure 6). The time to reach the peak value, however, does not seem to depend on the flow rate. Instead, the time to reach the peak is approximately the same for all

of the flow rates studied. After the peak has been reached, the area begins to decrease until it becomes steady and fluctuates around a constant level, which, in turn, is dependent on the flow rate. The time to reach the constant level also seems to be independent of the flow rate, but the amplitude of the fluctuation advances with the flow rate. The peak values of the open-eye area for flow rates of 200, 400 and 500 NL/min were 1.6 m^2, 3.2 m^2 and 5.0 m^2, respectively. The time-averaged values of the open-eye area were 0.69 m^2, 1.6 m^2 and 2.24 m^2.

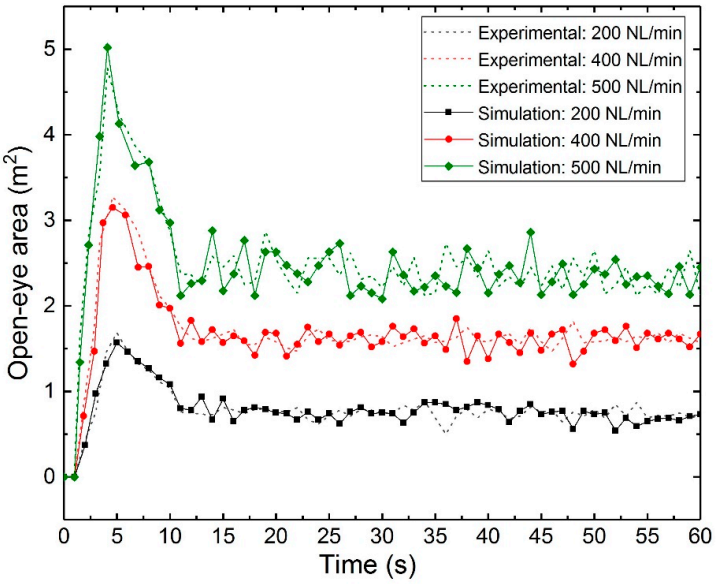

Figure 6. The dynamic open-eye area with time for experiments and simulation results.

Figure 7 depicts the flow velocity profiles at four different heights in the perpendicular direction where the flow enters from the porous plug. For all the flow velocity profiles at different heights, the highest mixture flow velocity occurred at the distance of 0.5 m from the vertical centre. This is the reason that the bubble plume developed from the argon gas injection through the porous plug located at this position. It can be seen from Figure 7 that the highest velocities (2.1–3.25) m/s for 200–500 NL/min) are obtained at the bottom of the ladle where the plume is quite narrow. At higher positions, the velocities decrease and the plume widens. The anticipated velocity fields follow the same trends in comparison to the experimental results of Xie et al. [35,36].

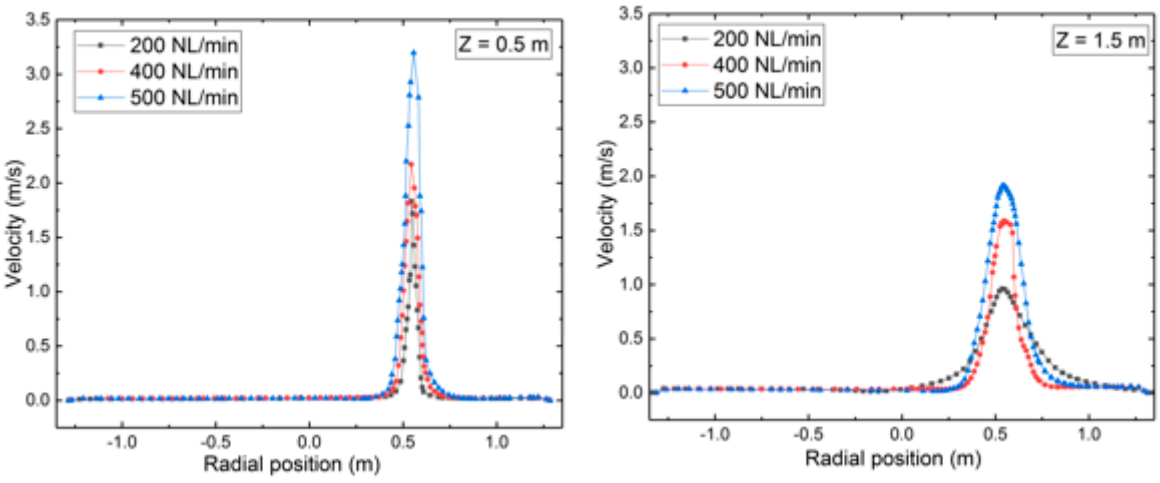

(**a**) (**b**)

Figure 7. *Cont.*

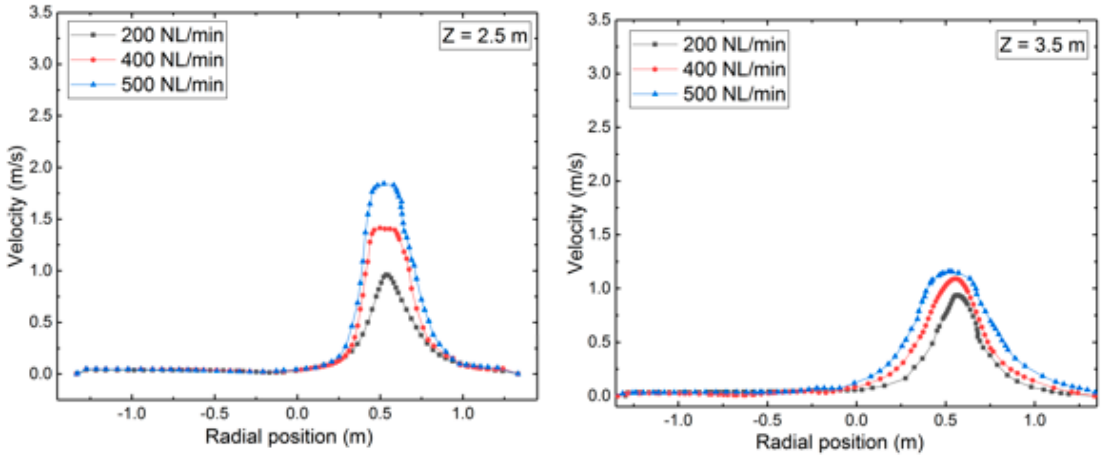

(**c**) (**d**)

Figure 7. Simulation results of time-averaged flow velocity profiles in the ladle furnace for different gas flow rates at different heights: (**a**) Z = 0.5 m, (**b**) Z = 1.5 m, (**c**) Z = 2.5 m, and (**d**) Z = 3.5 m.

Krishnapisharody and Irons [6] developed a mechanistic model for measuring the dimensionless open-eye size. The dimensionless open-eye area is expressed in terms of Froude number, which is further modified into the following correlation [31].

$$\frac{A_e^*}{A_p^*} = -3.0 + 13.78\,(1-\rho^*)^{-1/2}(Q^*)^{1/3}\left(\frac{H}{h}\right)^{1/2} \quad (8)$$

where $A_e^* = \frac{A_e}{H^2}$ (A_e^* is the non-dimensional open-eye area, A_e is the open-eye area and H is the bath height), $A_p^* = 1.41\,(Q^*)^{0.4}$ (A_p^* is the non-dimensional plume area, Q^* is the non-dimensional flow rate), $Q^* = \frac{Q}{g^{0.5}H^{2.5}}$ (g is the gravitational acceleration, Q is the gas flow rate), $\rho^* = \frac{\rho_{slag}}{\rho_{steel}}$ (ρ_{slag} is the density of the slag and ρ_{steel} is the density of the molten steel), h is the height of the slag layer) [31].

The anticipated trend of the dimensionless open-eye area showed acceptable agreement with the experimental results available from the literature. The experimental results of various authors and the meanings of the non-dimensional parameters in Figures 8 and 9 can be found in [6].

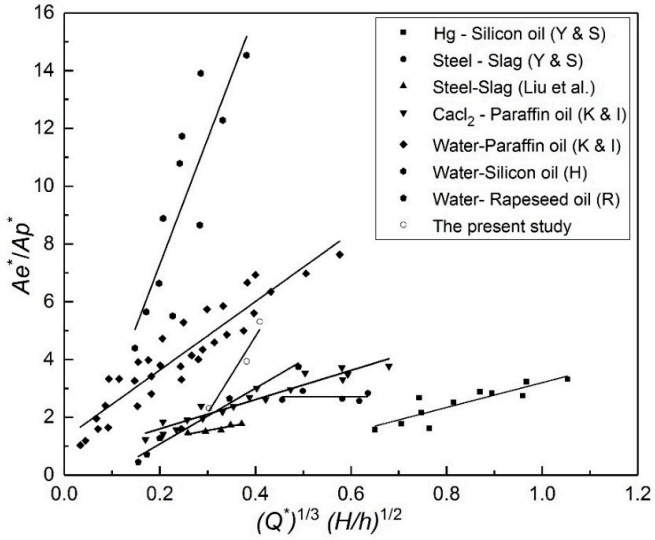

Figure 8. Comparison of non-dimensional open-eye area ratio with the literature (K & I: Krishnapisharody and Irons [6]; Yonezawa and Schwerdtfeger [5]; Han et al. [37]; E. Ramasetti et al. [36]: (A_e^*/A_p^*) *vs.* $(Q^*)^{\frac{1}{3}}\left(\frac{H}{h}\right)^{\frac{1}{2}}$).

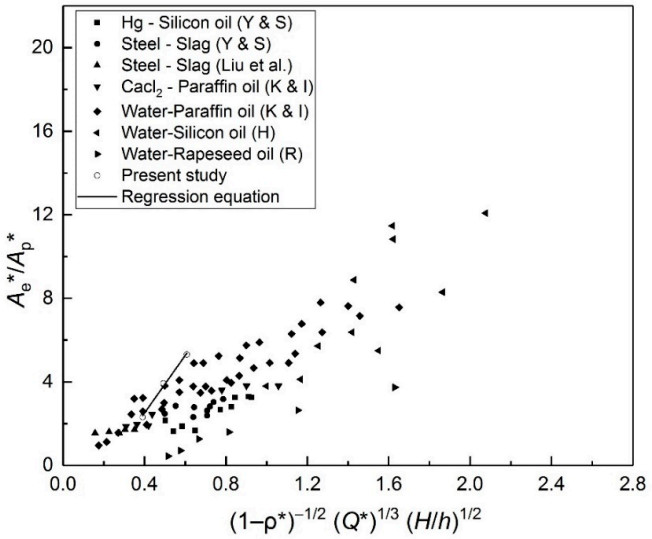

Figure 9. Comparison of the anticipated non-dimensional open-eye area ratio with dimensionless groups for gas injection (K & I: Krishnapisharody and Irons [6]; Yonezawa and Schwerdtfeger [5]; Han et al. [37]; Ramasetti et al. [36]: $\left(A_e^*/A_p^*\right)$ *vs.* $(1-\rho^*)^{-\frac{1}{2}}\left(Q^*\right)^{\frac{1}{3}}\left(\frac{H}{h}\right)^{\frac{1}{2}}$.

3.2. Influence of Increasing Slag Layer Height to 55 cm from 40 cm on Open-Eye Formation

Figures 10 and 11 display the influence of argon flow rate on the open-eye formation when the slag layer height was increased to 55 cm. At a low argon flow rate of 200 NL/min, increasing the slag layer thickness from 40 cm to 55 cm prevents the open-eye formation. The lowest argon flow rate was not high enough to break the slag layer during the experiments, which can be observed in Figure 8a and the same result was obtained in the simulations as well. This implies that it is necessary to decrease argon flow rates for higher slag layer thickness operating conditions to inhibit open-eye formation and to reduce inclusion formation by atmospheric reoxidation. This is because, according to the study of Valentin et al. [24], the inclusion content is larger when a open-eye is formed compared to the situation with a closed slag layer. At argon flow rates of 400 and 500 NL/min, open-eye formation follows the same trend as in the cases with a slag layer thickness of 40 cm, with a reduction in the open-eye size to some extent. At 400 NL/min, the open-eye area reduces from 1.58 m^2 (relative area of 23.3%) to 1.32 m^2 (relative area of 19.5%) in experimental results, and from 1.59 m^2 (relative area of 23.5%) to 1.44 m^2 (relative area of 21.1%) through simulation results. At 500 NL/min, the open-eye area reduces from 2.24 m^2 (relative area of 33.1%) to 1.81 m^2 (relative area of 26.7%) in experimental results, and from 2.29 m^2 (relative area of 34.0%) to 1.95 m^2 (relative area of 28.8%) through simulation results.

(**a**) (**b**) (**c**)

Figure 10. Open-eye size in the ladle from experimental results for a slag layer thickness of 55 cm: (**a**) Q = 200 NL/min, (**b**) Q = 400 NL/min, and (**c**) Q = 500 NL/min.

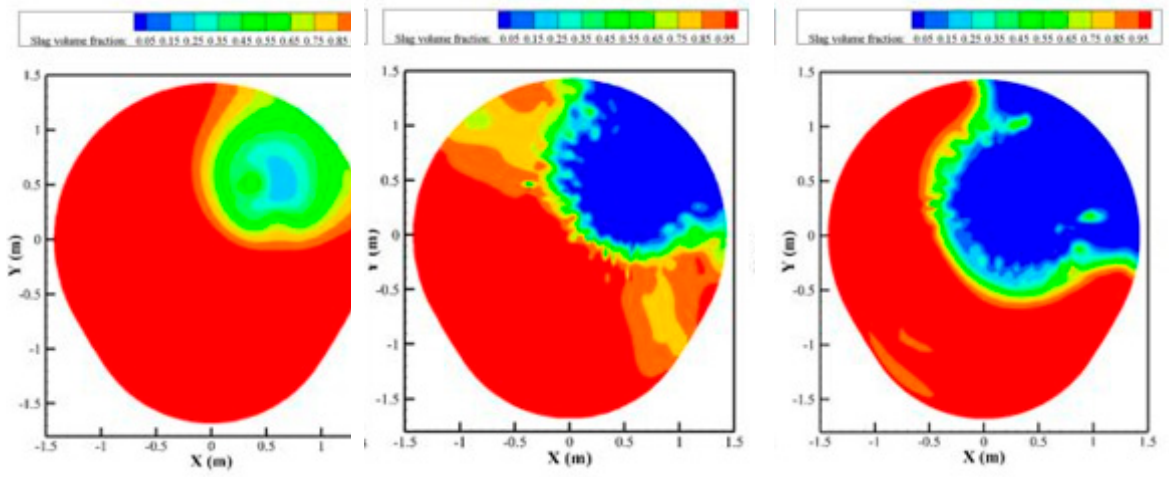

(**a**) (**b**) (**c**)

Figure 11. Open-eye size in the ladle from simulation results for a slag layer thickness of 55 cm: (**a**) Q = 200 NL/min, (**b**) Q = 400 NL/min, and (**c**) Q = 500 NL/min.

3.3. Influence of Decreasing Slag Layer Thickness to 25 cm from 40 cm on Open-Eye Formation

The open-eye formation in the ladle when the slag layer thickness was reduced to 25 cm for argon flow rates of 200, 400 and 500 NL/min is displayed in Figures 12 and 13. At argon flow rates of 200 and 400 NL/min, the open-eye formation follows the same trend as in the case of 40cm slag layer thickness, but with an increase in open-eye size. At a flow rate of 200 NL/min, the open-eye area enlarges to 1.08 m^2 (relative area of 15.9%) in experimental results and to 0.95 m^2 (relative area of 14.0%) through simulations when the slag layer height was decreased from 40 cm to 25 cm. In addition, at a flow rate of 400 NL/min, the open-eye area increases to 1.82 m^2 (relative area of 26.8%) in experimental results to 1.89 m^2 (relative area of 27.9%) through simulations. At a higher argon flow rate of 500 NL/min, the open-eye formation follows the same trend as in the case with a slag layer height of 40 cm, but the open-eye size is very large and there is a large deformation of the slag layer both near the open-eye position and far from it. The size of the open-eye is almost half of the ladle surface cross-sectional area. The results indicate that, the higher argon flow rates leads to the formation of larger open-eyes, and at high flow rates if the slag layer thickness is lower it may result in the generation of a fluctuating open-eye. Emulsification of slag into steel was found to be more aggressive compared to cases with gas flow rates of 200 and 400 NL/min.

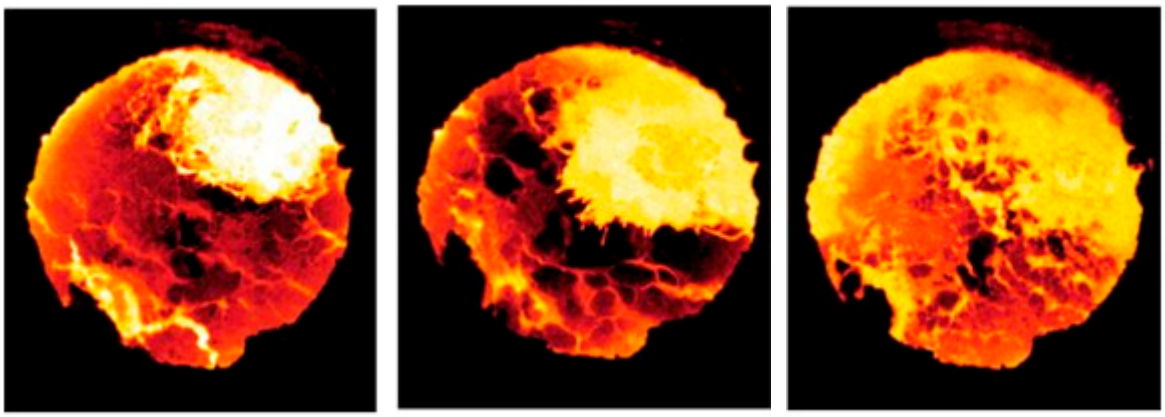

(**a**) (**b**) (**c**)

Figure 12. Open-eye size in the ladle from experimental results for a slag layer thickness of 25 cm: (**a**) Q = 200 NL/min, (**b**) Q = 400 NL/min, and (**c**) Q = 500 NL/min.

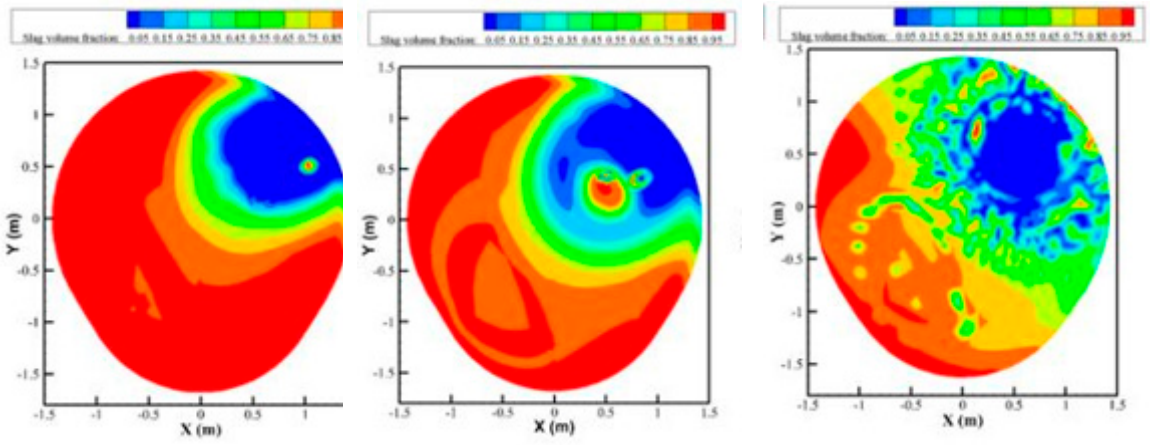

Figure 13. Open-eye size in the ladle from simulation results for a slag layer thickness of 25 cm: (**a**) Q = 200 NL/min, (**b**) Q = 400 NL/min, and (**c**) Q = 500 NL/min.

3.4. Summary of Open-Eye Area for Different Argon Flow Rates and Slag Layer Heights

Table 2 presents the summary of all the experimental and simulation results of open-eye areas for enlargement of flow rates from 200 to 500 NL/min and the slag layer height from 25 to 55 cm.

Table 2. Summary of experimental and simulated values for open-eye area with various gas flow rates and slag layer height.

Slag Layer Height (cm)	**25**		**40**		**55**	
Flow Rate (NL/min)	Exp. (m^2)	Sim. (m^2)	Exp. (m^2)	Sim. (m^2)	Exp.(m^2)	Sim. (m^2)
200	1.08	0.95	0.72	0.69	NA	NA
400	1.82	1.89	1.58	1.59	1.32	1.44
500	NA	NA	2.24	2.30	1.81	1.95
Average Relative Error			6.61%			
R^2			0.93			

Notes: NA = not available.

Overall, the open-eye area increases with elevation in flow rate and decreases with elevation in the slag layer height in experiments, while the same trend in also followed in the simulations. The low gas flow rate of 200 NL/min was not able to break the slag layer and generate an open-eye for a high slag layer height of 55 cm. The open-eye tended to be more dynamic when the ladle was operated with a high flow rate of 500 NL/min and a low slag layer height of 25 cm was used.

As expected, the open eye area expanded with a higher gas flow rate and diminished with a thicker slag layer. Figure 14 depicts the comparison between the experimental and simulation values of the open-eye area for different slag layer thicknesses. The agreement between the simulations and experiments is very good. The results indicate that the gas flow rate and slag layer height play an important role in generating a suitable open-eye size for alloying purposes. To keep the open eye constant, a thicker slag layer needs to be compensated for with a higher gas flow rate.

In industrial practice, the lower limit for the gas flow rate is set by the need to break up the slag layer. To maximize the yield of alloying materials it is necessary to have a sufficiently large open eye area to ensure that alloying materials end up in the metal phase. However, the upper limit is set by operating factors such as the cost of argon gas, the increased refractory wear induced by higher flow velocities, increased heat losses and oxidation through the open eye and increased inclusion formation.

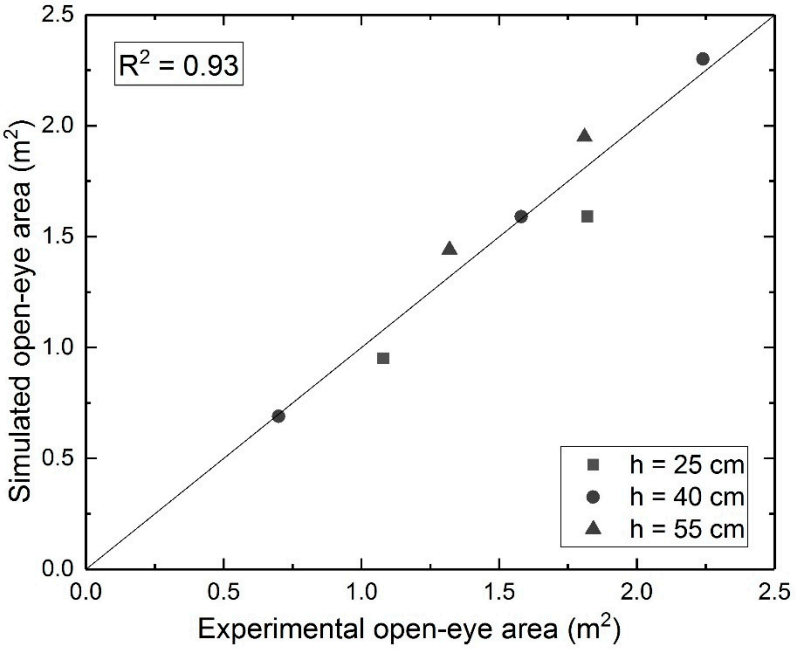

Figure 14. A comparison of experimental and simulated open-eye areas.

4. Conclusions

In this present study, the influence of argon flow rate and slag layer height on the fluid flow and open-eye formation in a 150 ton industrial scale ladle was investigated. The numerical model to simulate the multi-phase flow in the ladle was developed using the VOF model. To validate the model, the open-eye formation of an industrial ladle was captured using an IR camera. The simulated open-eye areas were found to be in good acceptance with the experimental footage and the CFD model developed has been verified by results measured in an industrial ladle. The results provide useful guidance for the selection of suitable flow rates and slag layer heights for operating industrial-scale ladles.

The following conclusions can be drawn from the experimental and simulation results:

(1) The injected argon flow rate has a significant influence on the fluid flow velocities and the open-eye size generated in the ladle.

(2) The elevation in flow rate of argon gas, the open-eye size and the spreading area of molten steel increases. The open-eye increases from 10.3% to 33.1% of the ladle's free top surface area with an increase of flow rate from 200 to 500 NL/min and a 40 cm slag layer thickness.

(3) The velocity of the fluid flow developed due to the injection of argon gas through the nozzle was very high adjacent to the nozzle inlet and reduces as the flow reaches the argon/steel/slag interface.

(4) The slag layer height has a great effect on the formation of the open-eye. The reduction of the slag layer thickness from 40 to 25 cm resulted in a much larger deformation of slag layer and a more rapidly fluctuating open-eye at a high flow rate of 500 NL/min. The increase of the slag layer thickness from 40 to 55 cm resulted in non-formation of an open-eye at 200 NL/min.

Author Contributions: Investigation: E.K.R.; methodology, J.S.; supervision, V.-V.V., P.S., M.L., T.F. and L.S.

Funding: The author is grateful to the European Commission for providing funding under grant number 675715–MIMESIS–H2020–MSCA–ITN–2015, which is part of the Marie Sklodowska-Curie Actions Innovative Training Networks European Industrial Doctorate Program.

Acknowledgments: Sapotech Oy support for capturing the open-eye formation process in the ladle at very high temperatures is thankfully acknowledged.

Conflicts of Interest: The authors declare no conflict of interest.

References

1. Yonezawa, K.; Schwerdtfeger, K. Spout eyes formed by an emerging gas plume at the surface of a slag-covered metal melt. *Metall. Mater. Trans. B* **1999**, *30*, 411–418. [CrossRef]
2. Yonezawa, K.; Schwerdtfeger, K. Height of the spout of a gas plume discharging from a metal melt. *Metall. Mater. Trans. B* **1999**, *30*, 655–660. [CrossRef]
3. Yonezawa, K.; Schwerdtfeger, K. Discharging of the spout of gas plumes discharging from a melt: Experimental investigation with a large-scale water model. *Metall. Mater. Trans. B* **2000**, *31*, 461–468. [CrossRef]
4. Krishnapisharody, K.; Irons, G.A. Modeling of slag eye formation over a metal bath due to gas bubbling. *Metall. Mater. Trans. B* **2006**, *37*, 763–772. [CrossRef]
5. Krishnapisharody, K.; Irons, G.A. Modeling of slag eye formation over a metal bath due to gas bubbling. *ISIJ Int.* **2008**, *48*, 1807–1809. [CrossRef]
6. Thunman, M.; Eckert, S.; Hennig, O.; Björkvall, J.; Sichen, D. Study of the Formation of Open-eye and Slag Entrainment in Gas Stirred Ladle. *Steel Res. Int.* **2010**, *78*, 849–856. [CrossRef]
7. Lv, N.N.; Wu, L.S.; Wang, H.C.; Dong, Y.C.; Su, C.J. Size analysis of slag eye formed by gas blowing in ladle refining. *J. Iron Steel Res. Int.* **2017**, *24*, 243–250. [CrossRef]
8. Amaro-Villeda, A.M.; Ramirez-Argaez, M.A.; Conejo, A.N. Effect of Slag Properties on Mixing Phenomena in Gas-stirred Ladles by Physical Modeling. *ISIJ Int.* **2014**, *54*, 1–8. [CrossRef]
9. Maruyama, A.; Iguchi, M. Cold model study of spout eye area in the presence of the slag layer simulated by low-density particles. *JSEM* **2012**, *12*, s7–s10.
10. Mazumdar, D.; Guthrie, R.I.L. Numerical computation of flow and mixing in ladle metallurgy steelmaking operations (C.A.S. method). *Appl. Math. Model.* **1986**, *10*, 25–32. [CrossRef]
11. Mazumdar, D.; Guthrie, R.I.L. On mathematical models and numerical solutions of gas stirred ladle systems. *Appl. Math. Model.* **1993**, *5*, 255–262. [CrossRef]
12. Mazumdar, D.; Yadhav, R.; Mahato, B. Transient flow and mixing in steelmaking ladles during the initial period of gas stirring. *ISIJ Int.* **2002**, *42*, 106–108. [CrossRef]
13. Mazumdar, D.; Guthrie, R.I.L. The physical and mathematical modelling of gas stirred ladle systems. *ISIJ Int.* **1995**, *35*, 1–20. [CrossRef]
14. Mazumdar, D.; Evans, J.W. A model for estimating exposed plume eye area in steel refining ladles covered with thin slag. *Metall. Mater. Trans. B.* **2004**, *35*, 400–404. [CrossRef]
15. Mandal, J.; Patil, S.; Madan, M.; Mazumdar, M. Mixing Time and Correlations for Ladles Stirred with Dual Plugs. *Metall. Trans. B* **2005**, *36*, 479–487. [CrossRef]
16. Patil, S.P.; Satish, D.; Peranadhanathan, M.; Mazumdar, D. Mixing Models for Slag Covered, Argon Stirred Ladles. *ISIJ Int.* **2010**, *50*, 1117–1124. [CrossRef]
17. Peranandhanthan, M.; Mazumdar, D. Modeling of Slag Eye Area in Argon Stirred Ladles. *ISIJ Int.* **2010**, *50*, 1622–1631. [CrossRef]
18. Li, L.; Liu, Z.; Li, B.; Matsuura, H.; Tsukihashi, F. Water Model and CFD-PBM Coupled Model of Gas-Liquid-Slag Three Phase Flow in Ladle Metallurgy. *ISIJ Int.* **2015**, *55*, 1337–1346. [CrossRef]
19. Li, L.; Li, B. Investigation of Bubble-Slag Layer Behaviors with Hybrid Eulerian-Lagrangian Modeling and Large Eddy Simulation. *JOM* **2016**, *68*, 2160–2169. [CrossRef]
20. Li, L.; Liu, Z.; Cao, M.; Li, B. Large Eddy Simulation of Bubble Flow and Slag Layer Behavior in Ladle with Discrete Phase Model (DPM)-Volume of Fluid (VOF) Coupled Model. *JOM* **2015**, *67*, 1459–1467. [CrossRef]
21. Liu, Z.; Li, L.; Li, B. Modeling of Gas-Steel-Slag Three-Phase Flow in Ladle Metallurgy: Part, I. Physical Modeling. *ISIJ Int.* **2017**, *57*, 1971–1979. [CrossRef]
22. Li, L.; Li, B.; Liu, Z. Modeling of Gas-Steel-Slag Three-Phase Flow in Ladle Metallurgy: Part II. Multi-scale Mathematical Model. *ISIJ Int.* **2017**, *57*, 1980–1989. [CrossRef]
23. Ramasetti, E.K.; Visuri, V.-V.; Sulasalmi, P.; Mattila, R.; Fabritius, T. Modeling of the Effect of the Gas Flow Rate on the Fluid Flow and Open-Eye Formation in a Water Model of a Steel Making Ladle. *Steel Res. Int.* **2019**, *90*, 1–12. [CrossRef]
24. Valentin, P.; Bruch, C.; Kyrylenko, Y.; Köchner, H.; Dannert, C. Influence of the Stirring Gas in a 170-t Ladle on Mixing Phenomena- Formation and On-line Control of Open-eye at an Industrial LD Steel Plant. *Steel Res. Int.* **2009**, *80*, 552–558.

25. Li, B.; Yin, H.; Zhou, C.Q.; Tsukihashi, F. Modeling of Three-phase Flows and Behavior of Slag/Steel Interface in an Argon Gas Stirred Ladle. *ISIJ Int.* **2008**, *48*, 1704–1711. [CrossRef]
26. Liu, H.; Qi, Z.; Xu, M. Numerical Simulation of Fluid Flow and Interfacial Behavior in Three-Phase Argon-Stirred Ladles with One Plug and Dual Plugs. *Steel Res. Int.* **2011**, *82*, 440–458. [CrossRef]
27. Cloete, S.W.P.; Eksteen, J.J.; Bradshaw, S.M. A Mathematical Modelling Study of Fluid Flow and Mixing in Full-Scale Gas-Stirred Ladles. *Prog in Comp Fluid Dyn.* **2009**, *9*, 345–356. [CrossRef]
28. Cloete, S.W.P.; Eksteen, J.J.; Bradshaw, S.M. A Numerical Modelling Investigation into Design Variables Influencing Mixing Efficiency in Full Scale Gas Stirred Ladles. *Miner. Eng.* **2013**, *46–47*, 16–24. [CrossRef]
29. Liu, W.; Tang, H.; Yang, S.; Wang, M.; Li, J.; Liu, Q.; Liu, J. Numerical Simulation of Slag Eye Formation and Slag Entrapment in a Bottom-Blown Argon-Stirred Ladle. *Metall. Trans. B* **2018**, *49*, 2681–2691. [CrossRef]
30. ANSYS Inc. *ANSYS Fluent Theory Guide*; Version 17; ANSYS Inc.: Canonsburg, PA, USA, 2009.
31. Ramasetti, E.K.; Visuri, V.-V.; Sulasalmi, P.; Mattila, R.; Fabritius, T. Physical and CFD modeling of the effect of top layer properties on the formation of open-eye in gas-stirred ladles with single and dual-plugs. *Steel Res. Int.* **2019**, *90*, 1900088. [CrossRef]
32. Valencia, J.J.; Quested, P.N. *ASM Handbook*; ASM International: Cleveland, OH, USA, 2008; pp. 468–481.
33. GTT Gesellschaft für Technische Thermochemie und –physik mbH. *FactSage*; Version 7.2; GTT Gesellschaft für Technische Thermochemie und –physik mbH: Sunnyvale, CA, USA, 2018.
34. Keene, B.J.; Mills, K.C. Densities of molten slags. In *Verein Duetscher Eisenhuttenleute: Slag Atlas*, 2nd ed.; Verlag Stahleisen GmbH: Düsseldorf, Germany, 1995; p. 313.
35. Xie, Y.; Oeters, F. Experimental studies on the flow velocity of molten metals in a ladle model at centric gas blowing. *Steel Res. Int.* **1992**, *63*, 93–104. [CrossRef]
36. Xie, Y.; Orsten, S.; Oeters, F. Behaviour of bubbles at gas blowing into liquid wood's metal. *Steel Res. Int.* **1992**, *32*, 66–75.
37. Han, J.W.; Heo, S.H.; Kam, D.H.; You, B.D.; Pak, J.J.; Song, H.S. Transient fluid flow phenomena in a gas stirred liquid bath with top oil layer-approach by numerical simulation and water model experiments. *ISIJ Int.* **2001**, *41*, 1165–1172. [CrossRef]